NAWCWPNS TP 8204

Experimental "Proof-of-Concept" of Phase Derivative Based Range Profile Enhancement ATR

by
Dave Banks
Erik van Bronkhorst
Dave Gagnon
Brett Borden
Research Department

AUGUST 1994

NAVAL AIR WARFARE CENTER WEAPONS DIVISION
CHINA LAKE, CA 93555-6001

Approved for public release; distribution is unlimited.

Naval Air Warfare Center Weapons Division

FOREWORD

The research described in this report was performed during the 1994 fiscal year as part of an effort to improve radar classification and identification capabilities for non-cooperative airborne targets. This problem continues to be a primary goal of radar research programs and considerable effort has been expended within the last few decades in attempts to solve it. The accuracy of these methods depends upon available radar resolution and so, indirectly, it depends on radar bandwidth.

A novel technique for radar-based non-cooperative target recognition has been created and verified using synthesized data. This current work has concentrated on verification of the method using measured data from scale model targets in an anechoic chamber. The method uses ordinary azimuth and elevation monopulse tracking data and is appropriate for application in many existing radar systems.

This effort was supported by ONR Code 1264 and by lab-discretionary (B&P) funds.

This report was reviewed for technical accuracy by Carey Schwartz.

Approved by
R. L. DERR, *Head*
Research Department
15 August 1994

Under authority of
D. B. McKinney
RAdm., U.S. Navy
Commander

Released for publication by
S. HAALAND
Deputy Commander for Research and Development

NAWCWPNS Technical Publication 8204

Published by .... Technical Information Department
Collation .... Cover, 5 leaves
First printing .... 35 copies

REPORT DOCUMENTATION PAGE

Form Approved OMB No. 0704-0188

1. AGENCY USE ONLY (Leave blank)

2. REPORT DATE
August 1994

3. REPORT TYPE AND DATES COVERED
Interim October 1993—March 1994

4. TITLE AND SUBTITLE
EXPERIMENTAL "PROOF-OF-CONCEPT" OF PHASE DERIVATIVE BASED RANGE PROFILE ENHANCEMENT ATR

5. FUNDING NUMBERS
N0001494WX35175

6. AUTHOR(S)
Dave Banks, Erik van Bronkhorst, Dave Gagnon, Brett Borden

7. PERFORMING ORGANIZATION NAME(S) AND ADDRESS(ES)
Naval Air Warfare Center Weapons Division
China Lake, CA 93555-6001

8. PERFORMING ORGANIZATION REPORT NUMBER
NAWCWPNS TP 8204

9. SPONSORING/MONITORING AGENCY NAME(S) AND ADDRESS(ES)
Office of Naval Research
Arlington, VA 22217-5000

10. SPONSORING/MONITORING AGENCY REPORT NUMBER

11. SUPPLEMENTARY NOTES

12A. DISTRIBUTION/AVAILABILITY STATEMENT
A Statement; Distribution Unlimited

12B. DISTRIBUTION CODE

13. ABSTRACT (Maximum 200 words)

(U) This report documents an initial effort to experimentally verify a novel automatic target recognition technique applicable to airborne radar targets. The method uses the information about the target's cross-range structure, which is statistically encoded in the radar tracking data and is potentially applicable to many existing radar missile systems.

14. SUBJECT TERMS
Radar, Range Profile, Target Recognition

15. NUMBER OF PAGES
10

16. PRICE CODE

17. SECURITY CLASSIFICATION OF REPORT	18. SECURITY CLASSIFICATION OF THIS PAGE	19. SECURITY CLASSIFICATION OF ABSTRACT	20. LIMITATION OF ABSTRACT
UNCLASSIFIED	UNCLASSIFIED	UNCLASSIFIED	UL

INTRODUCTION

Previously, a novel technique for extending the information available from range profiles of airborne radar targets has been developed and applied to the problem of automatic target recognition [References 1–4]. Since so much of the target shape information is tied up in the cross-range part of the radar "image", the principal difficulty with down-range profile techniques has been the limited target information available for classification purposes. Usual (e.g., Inverse Synthetic Aperture Radar, or ISAR) schemes are often unable to obtain this cross-range information because accurate association of aperture (induced by target motion) with data (collected over time) is very difficult [see Reference 3]. The alternate method that has been proposed uses data collected over an *unknown* aperture and does not require range-induced-phase adjustments across the set of measurements. In addition, the technique is not affected by aspect-induced scintillation. This statistical technique makes use of the fact that the spatial derivatives of the scattered field phase are independent of range-induced phase shifts and depend upon the cross-range extent of the target.

The present discussion reports on initial experimental efforts we have made to demonstrate the feasibility of the "enhanced range profile" technique. Using scale model targets in an anechoic chamber we have obtained very encouraging results which display the predicted features of the algorithm and show how the method might be applied to automatic target recognition (ATR) and aimpoint selection. We begin by reviewing the algorithm itself and developing the relevant ideas. Then we outline the measurement process and show some of our results.

BACKGROUND

Phase derivatives have been used for target tracking purposes for many years. So-called "phase monopulse" systems estimate the phase-gradient of the scattered field by differencing the outputs of closely-spaced antennas. The direction of this gradient will lie normal to surfaces of constant phase (phase fronts). When the target is a point scatterer the phase fronts will be spherical and centered on the target, and their normal directions will indicate target bearing. Of course, targets are not individual point scatterers and the phase-gradient will not always point to the target. The difference between actual target bearing and that estimated by the phase-gradient is known as target "glint error" and depends upon overall target structure.

A short radar pulse incident on a target can be used to isolate separate down-range target elements (see Figure 1). This is the idea behind range profiles, which are maps of scatterer reflectivity as a function of range. By combining short pulses with high resolution tracking, target subcomponent bearing directions can sometimes be determined as a function of range as well. Unfortunately, targets are usually sufficiently complex that each slice will generally contain more than one point scatterer and scintillation interference effects will still preclude accurate single-measurement bearing estimates—rather, statistical estimates based on multiple measurements are required.

When a set of phase derivative measurements are collected over a short time interval the effective aperture may be assumed to be small. If the target aspect cannot be accurately determined then

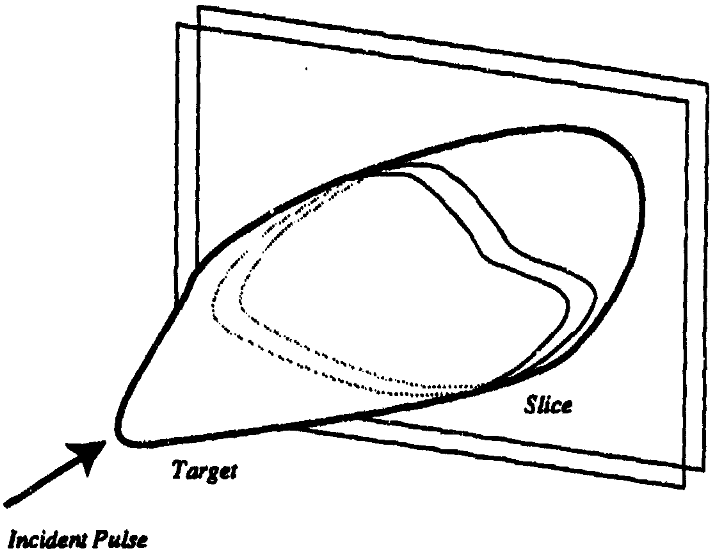

FIGURE 1. The Radar Pulse. A narrow radar pulse incident upon a target will illuminate only a range "slice" at any particular instant.

the glint error can be considered to be a function of random aspect angles. Let ϕ denote the phase of the scattered field so that $\mathbf{F}_{scatt} = |\mathbf{F}_{scatt}| \exp(i\phi)$. Then the cross-range component of the phase gradient along a direction θ (see Figure 2) is given by

$$g(\theta) \equiv (\hat{\imath}\cos\theta + \hat{\jmath}\sin\theta) \cdot \nabla\phi. \tag{1}$$

This will be the ideal measurement made by two closely spaced antennas lying along the θ direction.

At the high frequencies employed by typical phase monopulse "seekers" the phase factor ϕ will be a rapidly varying function of random aspect and its argument can be modeled as a uniform random variable on $(-\pi, \pi)$. Let $\rho(x, y)$ denote the local scattering reflectivity of the target at position (x, y) (see Figure 3). When the target is complex (the number of scattering centers is large) then the central limit theorem implies that $\mathbf{F}_{scatt}$ is normally distributed and, because of the distribution of the phase factor, has zero mean. The statistics of g follow from a straightforward, although somewhat lengthy, calculation [References 1,2,4]. The probability density of g is given by

$$f_g(g;\theta) = \frac{\kappa^2}{2(\kappa^2 + g^2)^{3/2}}, \tag{2}$$

where

$$\kappa^2(\theta) \equiv \int_{\mathbf{R}^2} |\rho(x', y')|^2 (x'\cos\theta + y'\sin\theta)^2 \, dx'dy'. \tag{3}$$

Equation (3) is the "second electrical moment" of the slice of target in the θ direction. Target shape information, in the form of scattering center moments weighted by local scatterer strength, can be deduced from a set of measured values of g by determining the parameter κ^2 that best fits

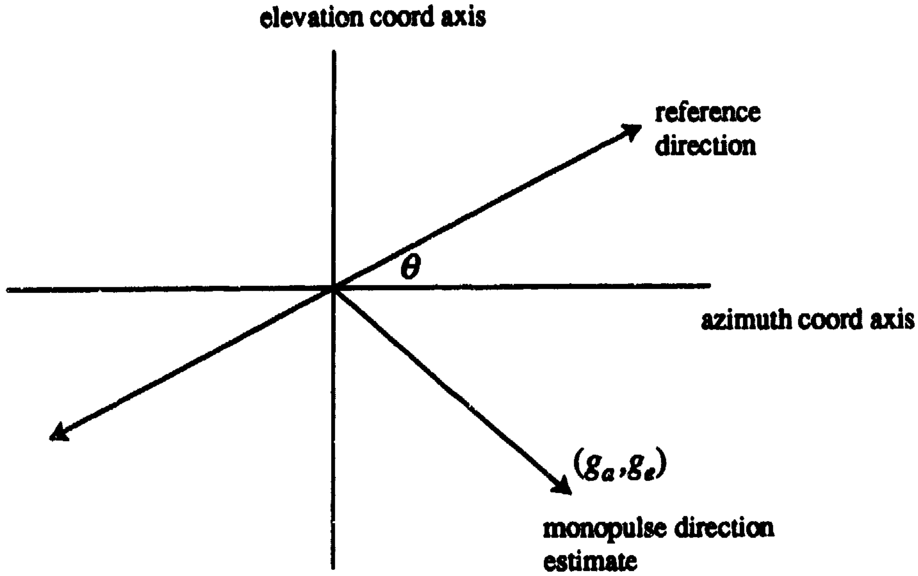

FIGURE 2. The Radar Coordinates. Here, $g_a \equiv g(\theta=0)$ and $g_e \equiv g(\theta=\pi/2)$ denote the components of the measured target bearing in the azimuth and elevation directions, respectively.

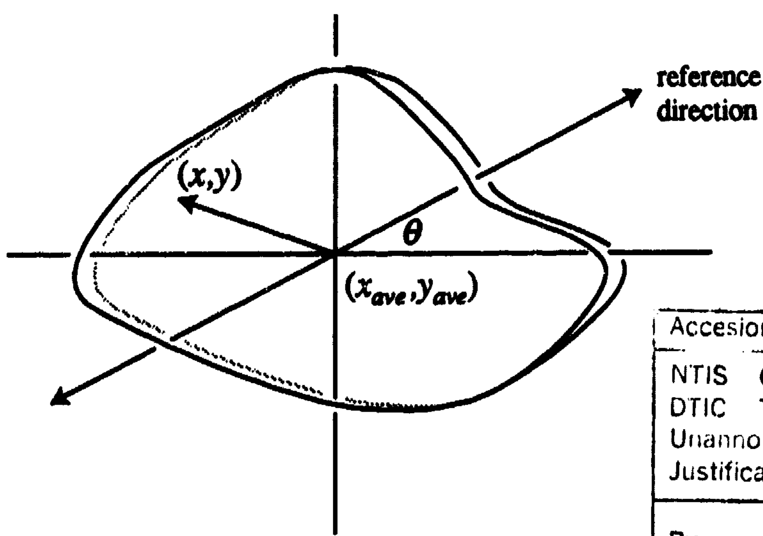

Figure 3. The Effective Target Slice.

the statistics of the data to the probability density of Equation (2). Moreover, it is easy to see that $\kappa(\theta) \equiv \sqrt{\kappa^2(\theta)}$ defines an ellipse whose shape and orientation depend upon the cross-range extent of the target. When combined with time-domain data acquired from a narrow pulse, Equation (3) will yield a family of down-range ellipses which will enhance ordinary down-range profiles by providing additional (although limited) cross-range target structure information.

The data used to estimate the "electrical moments of inertia" of an airborne target are the ordinary angle of arrival (AOA) measurements used in radar tracking systems. Since an airborne target will alter its orientation over time as it maneuvers (or, even if it is flying "straight and level") the AOA will fluctuate with time as well. (In the straight-flight case the target orientation will typically vary randomly over several degrees in only a few seconds and this results in significant variation in the AOA estimates.) The statistics of this variation are determined by the target orientation and the cross-range target structure in a known way. By fitting the statistics of the AOA measurements, collected over time, to this model, this cross-range information can be determined for each slice.

The resulting information obtainable is overall target orientation and moment "ellipse" estimates for each range slice (the moment ellipse has semi-axes defined by the electrical moments of inertia). In particular, each range slice is mapped to an ellipse which is itself defined by the five parameters described by Figure 4. The collection of all range slice ellipses associated with a target at a particular aspect defines the total available target structure and orientation information.

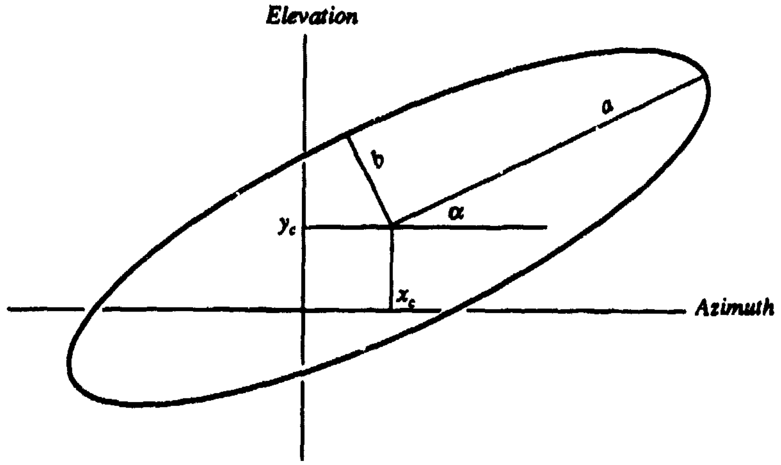

FIGURE 4. Ellipse Parameter Definition. These five parameters encode the cross-range target information available for each down-range slice.

Many existing radar tracking systems are capable of acquiring this data with only minor modification. For our purposes, and because of limited funding, we chose to collect sample data using the system described in Figure 5. An amplitude monopulse feed/comparator was attached directly to an HP-8510 network analyzer and used to collect frequency-domain data over a band of 42–48 GHz from a scale model target on a rotator in an anechoic chamber. The target was rotated through

2 degrees in azimuth and 3 degrees in elevation and was numerically transformed (DFT) into the time-domain as part of the preprocessing. Finally, 50 of these time-domain AOA measurement sets (corresponding to 50 randomly selected aspects from within the 2 degrees × 3 degrees measurement domain) were fed into the parameter fitting algorithm—the results from the target of Figure 6 are plotted in Figures 7–9.

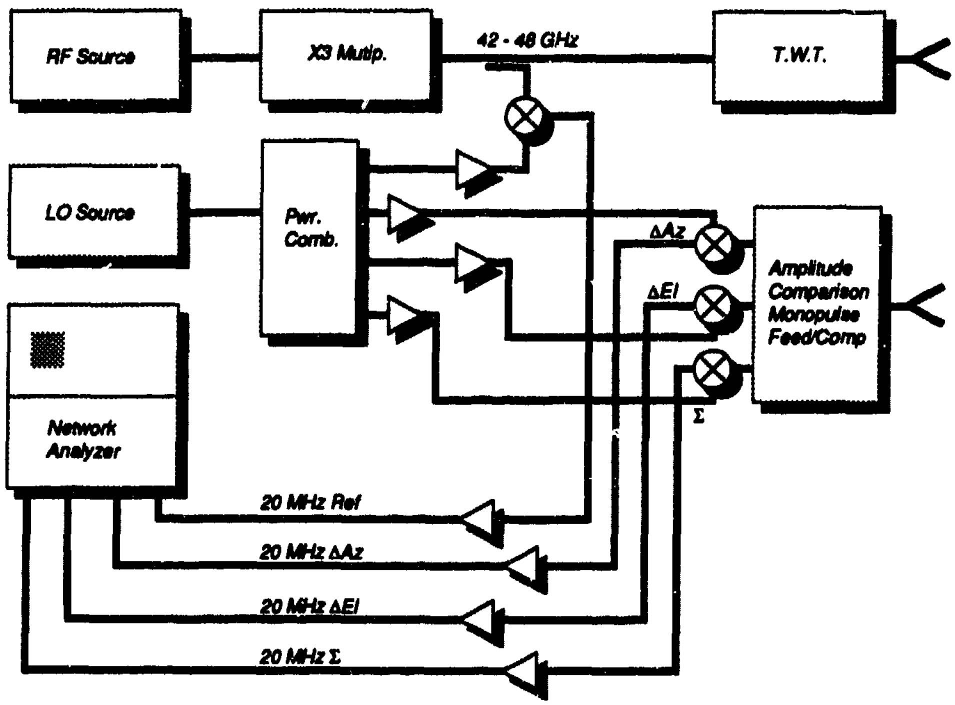

FIGURE 5. Angle of Arrival Measurement System.

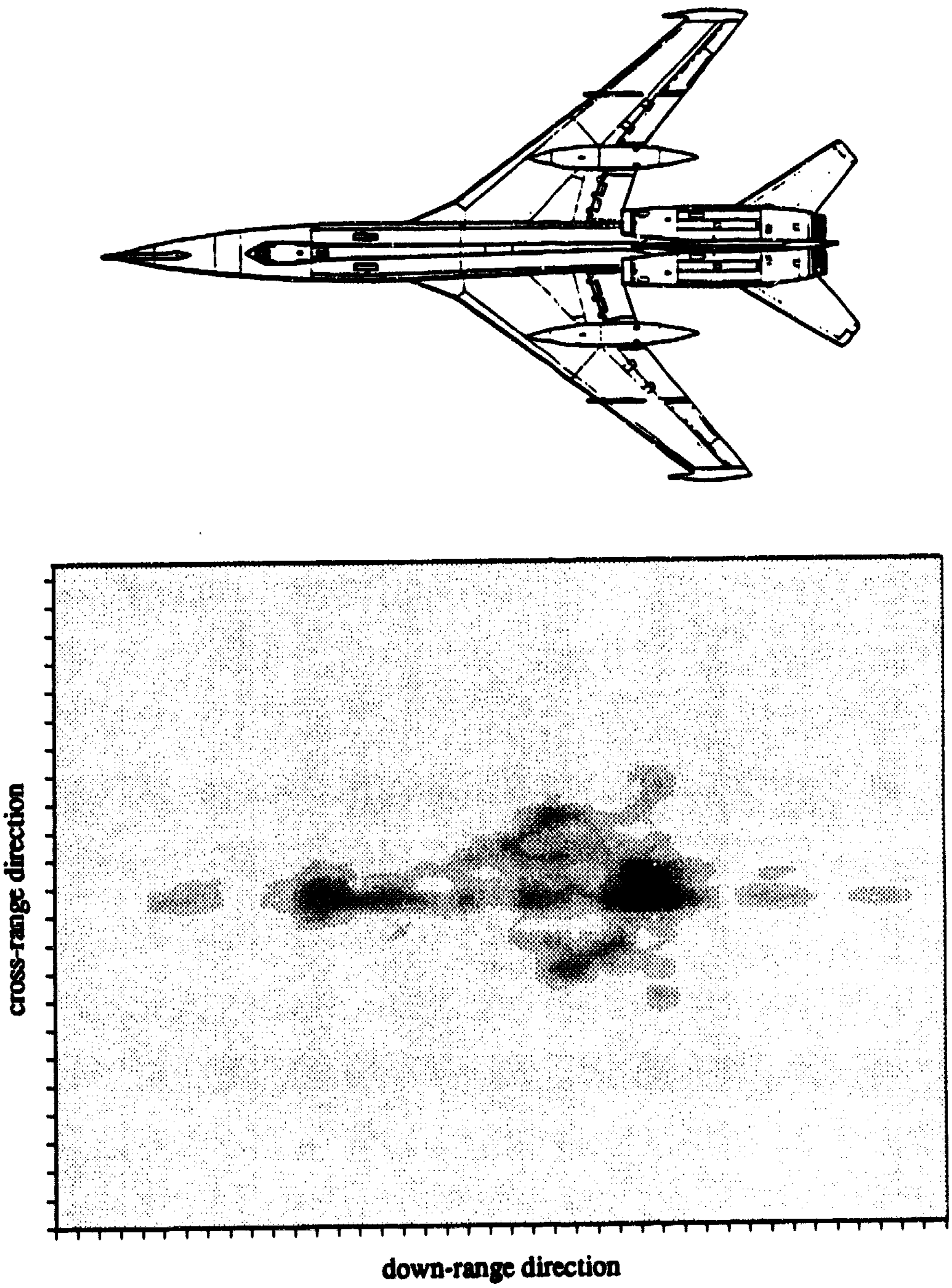

FIGURE 6. Sample Target (Tu-22 "Blinder") With Top-View ISAR Image of Electrically Active Elements.

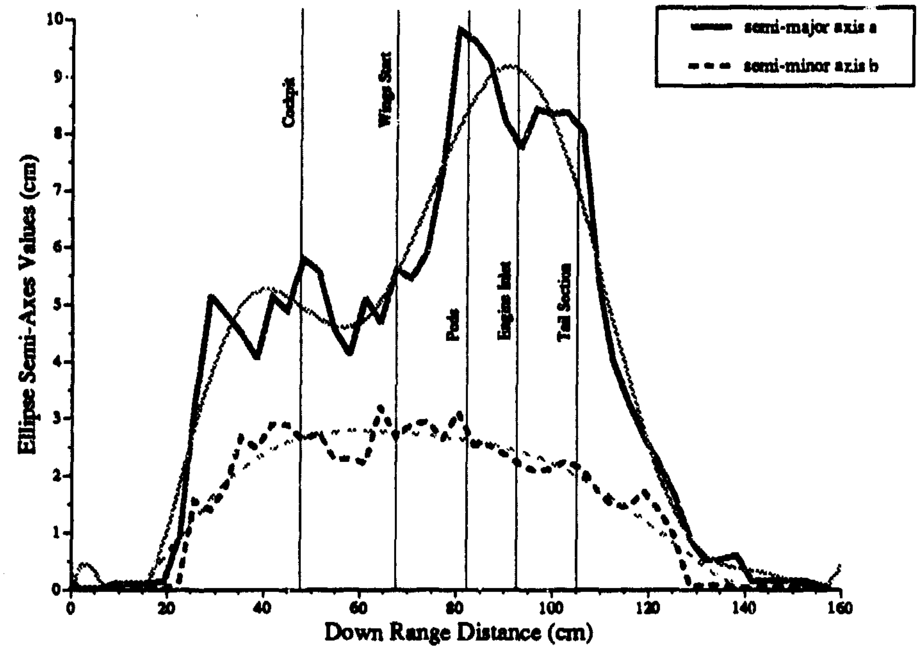

FIGURE 7. Enhanced Down-Range Profiles of a Scale Model Target. Shown are the cross-range semi-axes a and b of the "inertia" ellipses plotted as a function of range.

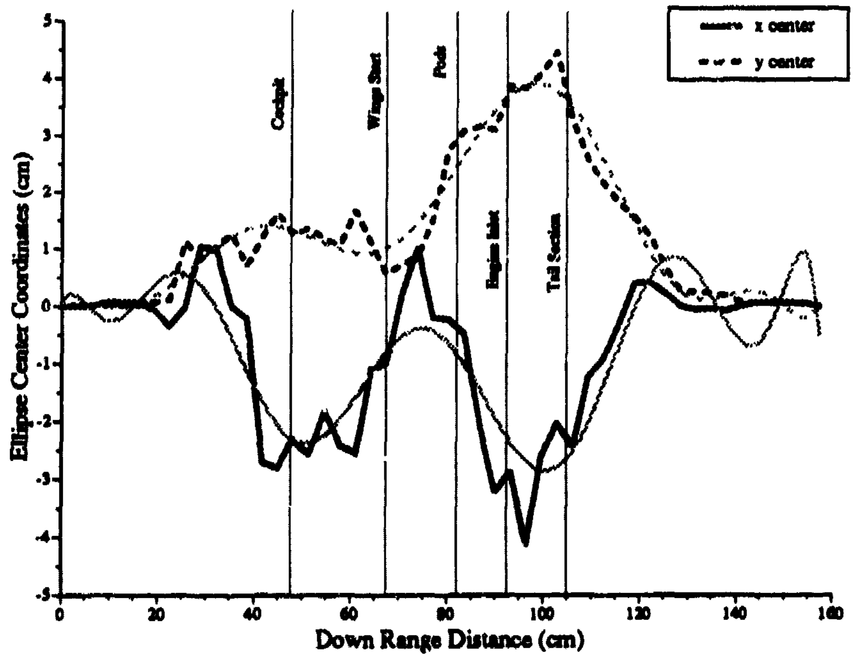

FIGURE 8. The Ellipse Center Coordinates x_c and y_c Plotted as a Function of Range.

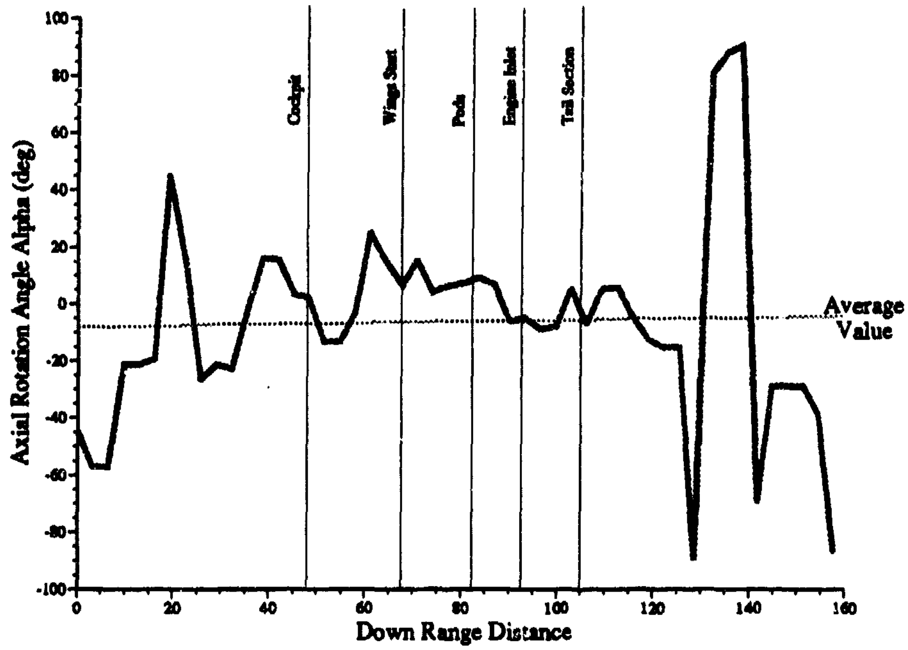

FIGURE 9. The Ellipse Orientation Angle α.

DISCUSSION

Because the anechoic chamber was small and precluded the use of large scale model targets, the conclusions that can be drawn from these results are limited. The target represented in Figure 6 was a 1/56 scale model Tu-22 ("Blinder") bomber and the radar system's center frequency and bandwidth scale to 800 MHz and 100 MHz, respectively. Consequently, the results are not nearly as good as should be expected from most currently deployed radar systems and full size targets.

To better appreciate these results we have included a high resolution ISAR image of the same scale model target using comparable data (in frequency and bandwidth) (Figure 6). This image defines the electrical target and contains all of the information available to the radar. Note that the target is electrically represented by less than about 20 scattering centers at the frequencies employed. This severely taxes the assumptions of the algorithm. In particular:

— The estimate of x_c is not constant along the target axis (as it should be ideally). This is because there were too few scattering centers to achieve a "good" average. Moreover, these errors also affect the semi-major axis estimates. Higher effective frequencies (as are appropriate to actual radar systems) will result in more effective scattering centers and so increased accuracy in parameter estimates.

— The target was dominated by the engine inlets. Since the cross-range ellipses are determined by intensity weighted averages of the scattering center position, the ellipse associated with this portion of the target is much more narrow that would be expected by a casual inspection of the target model.

In fact, the overall target is electrically much more narrow than it is physically. (Note that the wings are not electrically active beyond the pods.) Since so much of the strong features are concentrated along the center of the target, this makes it difficult to interpret the data results, which contain such small variation.

Nevertheless, the results of Figures 7–9 clearly demonstrate the effectiveness of the algorithm *even for this worst-case test*. The target orientation has been accurately estimated as well as the overall target shape and structure.

CONCLUSIONS AND RECOMMENDATIONS

We do not feel comfortable claiming the algorithm as "proved effective for ATR." Rather, because of the limitations in the test we have only demonstrated that the algorithm is remarkably effective even when the model assumptions are significantly relaxed. In particular, the technique is clearly appropriate for the more limited problem of aim-point selection in rf-guided missiles. In fact, because the identical data are also used for guidance, this method may prove to be an optimal (practical) aim-point selection algorithm.

A more complete demonstration of the method (for ATR) will require larger model targets with more realistic complex structures. However, given the relative success so-far, as well as the experience gained in the current effort, a complete and convincing demonstration should be straight forward.

REFERENCES

1. B. Borden. "High-frequency statistical classification of complex targets using severely aspect-limited data," *IEEE Trans. on Antennas and Prop.*, Vol. 34 (1986), 1455
2. B. Borden. "Phase monopulse tracking and its relationship to non-cooperative target recognition," *IMA Volumes in Mathematics and its Applications, Radar and Sonar, Part 2, Vol. 39*, edited by F. A. Grunbaüm, M. Bernfeld and R. E. Blahut. New York, Springer-Verlag, 1992
3. B. Borden. "Problems in airborne radar target recognition," *Inverse Problems*, (to appear in 1994)
4. B. Borden. "Enhanced down-range profiles for wideband radar-based target classification using phase-front derivative statistics," *IEEE Trans. on Antennas and Prop.*, (to appear in 1994)

INITIAL DISTRIBUTION

5 Naval Air Systems Command, Arlington
  AIR-5117E (1)
  AIR-5164
    File (1)
    Stegman (1)
  AIR-526 (1)
  PMA-235 (1)
2 Defense Technical Information Center, Alexandria
2 Center for Naval Analyses, Alexandria, VA
  Dr. A. Borden (1)
  L. Lynn (1)

ON-SITE DISTRIBUTION

1 Code C0231, S. Chesnut
10 Code C02313, B. Borden
1 Code C0252, T.Loftus
1 Code C2156, W. Katzenstein
1 Code C2158, D. Reade
1 Code C2822, D. Paolino
1 Code C29A4, G. Winkler
1 Code C29B5, M. Mumford
1 Code C291, R. Smith
1 Code C2911, G. Hewer
4 Code C643 (3 plus Archives Copy)